

LoS-Map Construction for Proactive Relay of Opportunity Selection in 6G V2X Systems

Francesco Linsalata, *Student Member, IEEE*, Silvia Mura, *Student Member, IEEE*,
 Marouan Mizmizi, *Member, IEEE*, Maurizio Magarini, *Member, IEEE*, Peng Wang, *Member, IEEE*,
 Majid Nasiri Khormuji, *Senior Member, IEEE*, Alberto Perotti, *Senior Member, IEEE*,
 Umberto Spagnolini, *Senior Member, IEEE*

Abstract—Recent advances in Vehicle-to-Everything (V2X) technology and the upcoming sixth-generation (6G) network will dawn a new era for vehicular services with enhanced communication capabilities. Connected and Autonomous Vehicles (CAVs) are expected to deliver a new transportation experience, increasing the safety and efficiency of road networks. The use of millimeter-wave (mmW) frequencies guarantees a huge amount of bandwidth ($>1\text{GHz}$) and a high data rate ($>10\text{Gbit/s}$), which are required for CAVs applications. However, high frequency is impaired by severe path loss, and line of sight (LoS) propagation can be easily blocked by static and dynamic obstacles. Several solutions are being investigated, and the most promising one exploits relays. However, traditional relay schemes react to link failure and leverage instantaneous information, which impedes efficient relay selection in highly mobile and complex networks, such as vehicular scenarios. In this context, we propose a novel proactive relaying strategy that exploits the cooperation between CAVs and environment information to predict the dynamic *LoS-map*, which describes the links' evolution in time. The proactive relaying schemes exploit the dynamic *LoS-map* to maximize the network connectivity. A novel framework integrating realistic mobility patterns and geometric channel propagation models is proposed to analyze the performance in different scenarios. Numerical simulations suggest that the proactive relaying schemes mitigate beam blockage and maximize the average probability of connecting CAVs with reliable links.

Index Terms—6G, V2X, CAV, mmW, relay selection

I. INTRODUCTION

CONNECTED and Automated Vehicle (CAV) technology will revolutionize the transportation system by providing a safer, more efficient, and less polluted road environment. CAV's main distinguishing features are the availability of various on-board sensors (e.g., Lidar, Radar, cameras, etc.) for environment perception and the enhancement of the Vehicle-to-Everything (V2X) communication capabilities [1, 2]. Current V2X systems are mainly based on two alternative radio access technologies: i) Dedicated Short Range Communications (DSRC) sponsored by IEEE [3] and ii) Cellular V2X (C-V2X) promoted by the 3rd Generation Partnership Project (3GPP) [4]. Both standards operate at sub-6 GHz

frequencies, i.e., Frequency Range 1 (FR1), and can only meet the requirements of basic V2X services due to the limited bandwidth [5]. 6G V2X is expected to support a wide range of services, i.e., enhanced-V2X (e-V2X), with increasingly stringent requirements: $>10\text{Gbps}$ per link, $<1\text{ms}$ latency, and $<1\cdot 10^{-9}$ reliability [6]. To address these new demands, the 3GPP has launched 5G New Radio (NR) V2X Rel. 16 [7] and further enhancements from Rel. 17 [8] are under discussion. The most significant innovation in Rel. 17 is the possibility of exploiting mmW frequencies (24.25 GHz-52.6 GHz), i.e., Frequency Range 2 (FR2), to support bandwidth-demanding applications. Furthermore, sub-THz (90-300 GHz) are being studied for 6G V2X communications [9].

Propagation at such high frequencies is subject to severe attenuation and mostly requires an LoS condition. Indeed, blockage is the most relevant limitation for the range covered and for communication reliability [10]. Massive Multiple-Input Multiple-Output (MIMO) systems are promising solutions for high-frequency communication, enabling a beam-type communication capable of achieving high antenna gain. Beam alignment and tracking are key issues, mostly in a dynamic environment as in vehicular scenarios, where frequent beam misalignments and blockages occur, with a detrimental effect on the system's performance [11].

Beam blockage can be mitigated by relaying mechanisms [12, 13], for example, from nearby CAVs, Road Side Units (RSU), or Intelligent Reflecting Surfaces (IRS) [14]. Relay selection strategies can be grouped into two macro-categories: i) centralized [15, 16]: a network entity, such as Next Generation Base Station (gNB) or an elected vehicle, acts as a *central body* (CB) that collects network state and defines the optimal relay selection; ii) distributed [13, 17]: each vehicle computes the ego optimal relay and attempts to directly interact with it. Relay selection algorithms require fresh and updated information regarding the network to optimally allocate the relaying resources. These operations introduce delays and require signaling. In the mmW vehicular scenario, the network information is outdated rapidly due to the high mobility [18], yielding the relay selection inefficient. Moreover, multi-hop links are subject to a higher blockage probability compared to direct links. In this context, we design a novel criterion for dynamic LoS-map prediction and propose a novel framework for relay of opportunity selection to enable high-quality and stable V2X links. Relay selection is based on cooperative sensing to cope with LoS blockage conditions.

F. Linsalata, S. Mura, M. Mizmizi, and M. Magarini are with Dipartimento di Elettronica, Informazione e Bioingegneria, Politecnico di Milano, Via Ponzio 34/5, 20133, Milano Italy.

P. Wang, M. N. Nasiri, and A. Perotti are with Huawei Technologies Sweden AB, Skalholtsgatan 9-11, SE-164 94 Kista, Stockholm, Sweden

U. Spagnolini is with Dipartimento di Elettronica, Informazione e Bioingegneria, Politecnico di Milano, Via Ponzio 34/5, 20133, Milano Italy and Huawei Industry Chair.

Related Works

Many works in literature approach relay selection by abstracting the physical layer. The authors in [19] propose a distributed vehicular relay selection strategy assuming a Nakagami fading channel. A moving-zone-based architecture is proposed in [16], where the CB is elected from the set of vehicles and it establishes a connectivity with the closest relay to the destination by using the Dijkstra algorithm. In [20] the channel state information at the communication antenna is predicted based on a predictor antenna, which is a second antenna mounted on the CAV's front bumper. The presence of a predictor antenna can boost the relaying communication performance. However, the prediction time horizon depends on the speed of the CAV and the distance between predictor and communication antennas, which is limited by the size of the CAV. Relaying in vehicular networks perspective has been extensively studied [21, 22, 23]. In particular, the authors in [22] proposed two relay schemes to extend the transmission range in a vehicular platooning application. The investigated approaches select the relay based on the geographic location information, showing a significant reduction in the outage probability compared to the single relay case. A multi-relay scheme is proposed in [24], where the base stations cooperate as relays to support vehicular communication, leveraging on the geographical location information. The authors in [25] suggest the deployment of relay nodes in the network to support vehicular communication. Different relaying schemes are compared under different nodes density/deployment scenarios, considering instantaneous and average Signal to Noise Ratio (SNR) and data rate as selection bases.

In [26], the authors assume that each vehicle equipped with a GPS receiver can download the digital maps from the cloud. Their combination can be used to choose from the neighbors a relay node that is strategically located in the perfect-reception zone.

In order to overcome the LoS blockage problem at mmW, in [27] the authors propose using neighbouring vehicles as relays to forward the blocked traffic flows. Specifically, a traffic-aware relay vehicle selection is investigated, by combining the results of an analytic hierarchy process and coalitional game. A heuristic relay selection scheme is devised to select the relay vehicle with the best rationality degree. However, these works investigate solutions in simplified road traffic scenarios at sub-6GHz frequencies, without capturing the full complexity of dense vehicular environments and the harder propagation at mmW frequencies. Moreover, they assume the absence of old branded non connected cars that naturally interrupt the links. Moreover, a common limitation of the works concerning the relay-assisted mmW V2X communications is the widespread use of stochastic models of the channel. This is very limiting in modelling the complex real-world scenario. For example, stochastic channels do not account for the impact on the system's performance of *dynamic* blockers, such as moving vehicles.

In [28], the authors use a Network Simulator 3 (NS-3) [29] mmW module and 5G Lena [30] for simulating V2I communication, focusing only on cellular-like and infrastructure-based

deployments. Coverage, mobility, and blockage are studied in [31] by exploiting a 3D ray-tracer to accurately reproduce the mmW channel propagation [32]. The simulation architecture achieves high performance in replicating the channel propagation model but its high complexity fails to capture the insight of the dynamics for relay scheduling design.

Contributions

This paper is contextualized in the future 6G-enabled CAV applications/services where CAVs share sensor data to improve the perception of the surrounding environment. CAVs are equipped with two communication interfaces: mmW beam-type communication for high data rate and a sub-6 GHz for signalling and control [33] as depicted in Fig. 1a. This paper's main contributions can be summarized as follows:

- The proposed approach leverages on cooperative sensing to predict the LoS-map of the V2X network and to design a countermeasure to beam blockage. The static objects (e.g., buildings and trees) in the LoS-map can be retrieved either from the 3D maps downloaded from edge server or by the CAVs' on-board sensors. The trajectories of dynamic objects, such as non-cooperative vehicles, are derived by reshaping the motion prediction algorithm in [34]. The vehicles' mobility and the uncertainty on the objects' position lead to dynamic LoS conditions, which depends on the traffic density, and impacts on the corresponding V2X connectivity.
- The distribution of the LoS-map is derived analytically for V2X scenarios. Instantaneous network connectivity for a dynamic vehicular mesh is evaluated in the conditions of no relaying (lower bound), and optimal relaying (upper bound), i.e., all CAVs can act as relays with unlimited resources. This enables the comparison of different relaying techniques, both centralized and distributed, under various link and traffic conditions.
- A unified simulation methodology of mmW V2X networks is proposed. The modelling of vehicle traffic over real road networks is obtained by using a combination of OpenStreetMap (OSM) [35] and Simulation of Urban MObility (SUMO) [36] software. Furthermore, the output of SUMO is processed by the Geometry-based, Efficient Propagation Model for Vehicle-to-Vehicle (GEMV²) [37] software, in which the radio propagation has been adapted according to the latest 3GPP guidelines in [38]. All numerical results are based on this integrated simulation environment.

Organization

The rest of this paper is organized as follows. Section II introduces the methodology, while Section III deals with the network connectivity analysis. Section IV gives an overview of centralized relay selection schemes, while Section V focuses on the distributed relay selection schemes. Section VI describes the implemented simulation set-up with scenario definition and the CAVs' data sharing studied cases. Numerical results and complexity analysis are investigated in Section VII. Lastly, Section VIII summarizes and concludes the work.

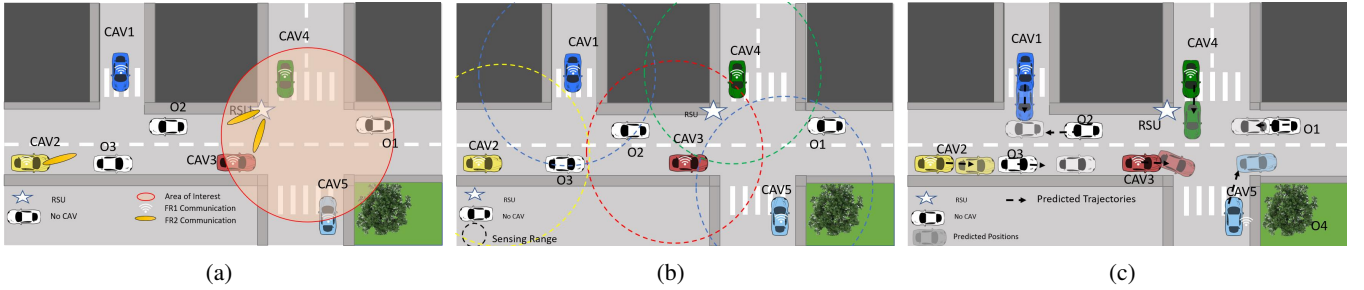


Figure 1: V2X extended sensing between RV (e.g. yellow and blue car) and VoI (e.g. red and green cars). In (a) the scenario at the collection phase instant, in (b) the Cooperative Awareness Signalling to enable cooperative sensing, and in (c) the predicted trajectories based on CA signalling and maneuvers- and physical-based models.

Notation

Bold upper and lower-case letters describe matrices and column vectors, respectively. $[\mathbf{A}]_{(i,j)}$ denotes the (i, j) entry of matrix \mathbf{A} . Transposition and conjugate transposition are denoted with the operator $(\cdot)^T$ and $(\cdot)^H$, respectively. The determinant of matrix \mathbf{A} is $\det(\mathbf{A})$. $|\cdot|$ is the cardinality of a matrix or a set, i.e. its number of elements. With $\mathbf{a} \sim \mathcal{CN}(\boldsymbol{\mu}, \mathbf{C})$ we denote a multi-variate complex Gaussian random variable \mathbf{a} with mean $\boldsymbol{\mu}$ and covariance \mathbf{C} . \mathbf{I}_M stands for the identity matrix of dimensions $M \times M$, and $\mathbf{1}_M$ is the all-ones vector of dimensions $1 \times M$. The functions $f_X(x)$ and $F_X(x)$ define the probability density function (pdf) and cumulative density function (cdf) of a random variable X , respectively. The notation $m^{(i,j)}$ is used to indicate a metric m of the link between the (i, j) th communication couple, while p^i associates the parameter p to the i th CAV, RSU, and/or object.

II. METHODOLOGY

This section introduces the proposed methodology for the selection of the relay of opportunity based on a prediction of the LoS-map. First, the upcoming network state is estimated by leveraging the static information and cooperative perception of CAVs. Then, the predicted links' availability, i.e., the probability that the SNR is higher than a predefined threshold, is used for relay selection schemes.

A. Study Case

CAVs are assumed to be equipped with two communication interfaces: *i*) a low data-rate and omnidirectional communication interface for Cooperative Awareness (CA) messages, dissemination and signalling (e.g., 5G NR in FR1); *ii*) a high data-rate and beam-based communication interface for raw sensor data sharing (e.g., 5G NR in FR2 or 6G Sub-THz). Moreover, each CAV is assumed to share its planned trajectory with nearby CAVs.

Figure 1 depicts the considered scenario with sketched beams. We consider V2X extended sensing as the 3GPP use case [38]. The CAVs exchange raw or nearly raw sensor data to achieve an augmented perception. More specifically, a Requesting Vehicle (RV) can establish direct access to the sensor of a Vehicle of Interest (VoI) after creating an Over-the-Air data bus, or virtual data bus [39] for sensor' data

exchange. A CAV that is approaching a certain critical area, e.g., road intersection or roundabout, requires an augmented perception of the objects/obstacles present in the scene and their state to perform a safe manoeuvre. By referring to Fig. 1a, we denote the critical area as the Area of Interest (AoI), the collaborating CAVs as VoI (e.g., green and red cars in Fig. 1a), and the approaching CAVs as RVs (e.g., blue and yellow cars in Fig. 1a). The VoIs inside the intersection (or roundabout) possess an advantageous point of view of that road segment's traffic flow. The incoming vehicles (i.e., RVs), on the other hand, are entering a critical road area, and need to gather as much perceptive information as possible.

B. Cooperative LoS-map Sensing

The on-board sensing of each CAV perceives the surrounding static and dynamic blockers at a specific time instant t_0 . The mutual positioning is then exchanged using the FR1 communication interface to obtain the cooperative sensing of the objects. The signalling to accomplish cooperative sensing has been standardized by the Intelligent Transportation System (ITS) society for CAVs, mainly for safety-related use cases. According to 3GPP [40], vehicles can exploit three types of Cooperative Awareness (CA) signaling: Cooperative Awareness Message (CAM), Decentralized Environmental Notification Message (DENM), and Cooperative Perception Messages (CPM). CAMs enable mutual awareness between CAVs and detected obstacles, DENMs are event-based messages containing information related to a road hazard or abnormal traffic conditions, and CPMs contain self-information, such as the available on-board sensors, sensors range, sensors field of view, position, speed, heading, and size of the detected objects.

In particular, for each detected object k at time instant t_0 , the i th CAV estimates its position $(\tilde{x}_i^k(t_0), \tilde{y}_i^k(t_0))$ and speed $\tilde{v}_i^k(t_0)$ along x and y directions of the Cartesian plane. These parameters define the state of the k th object, which is represented as the column vector

$$\tilde{\mathbf{s}}_i^k(t_0) = [\tilde{x}_i^k(t_0), \tilde{y}_i^k(t_0), \tilde{v}_{i,x}^k(t_0), \tilde{v}_{i,y}^k(t_0)]^T \quad (1)$$

that due to the measurement uncertainty can be approximated as $\tilde{\mathbf{s}}_i^k(t_0) \sim \mathcal{N}(\mathbf{s}_{true}^k(t_0), \tilde{\boldsymbol{\Sigma}}_i^k(t_0))$ where $\mathbf{s}_{true}^k(t_0)$ is the true state of the k th object [41].

The list of K objects $\mathcal{L}_i = \{\tilde{\mathbf{s}}_i^1(t_0), \dots, \tilde{\mathbf{s}}_i^K(t_0)\}$ sensed by the i th CAV and their spatial footprint (see Remark 1) are

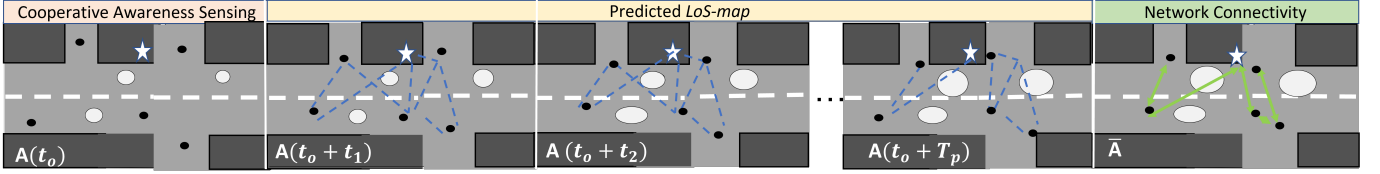


Figure 2: V2X network evolution while moving: after sensing, each CAV knows the others' state (black dots); the metrics based on predicted trajectories (black for CAV and white dots for old branded cars) are used to build an adjacency matrix $\mathbf{A}(t)$ for each time instant t . The entries of $\mathbf{A}(t)$ represent the service probability of the communication links involving CAVs and RSU, and it depends on the SNR.

signalled by leveraging on CA messages through the FR1 interface.

An estimate of the state associated with the k th object is obtained by each CAV (for a distributed architecture) after reaching cooperative consensus or by the CB (in case of a centralized architecture). Assuming the presence of N_c CAVs, the initial state of the k th object is approximated as

$$\tilde{\mathbf{s}}^k(t_0) \sim \mathcal{N}(\mathbf{s}_{true}^k(t_0), \tilde{\Sigma}^k(t_0)), \quad (2)$$

where the covariance matrix is

$$\tilde{\Sigma}^k(t_0) = \left(\sum_{i=1}^{N_c} \tilde{\Sigma}_i^k(t_0)^{-1} \right)^{-1}. \quad (3)$$

In the proposed framework, the CA signalling at FR1 is exploited to enable the communication at mmW frequency (e.g., in Fig. 1b). In fact, by combining the CA-based information and the blockers states, each CAV can evaluate its static LoS-map at t_0 and predict the dynamic LoS-map in the interval $[t_0, t_0 + T_p)$, estimating the LoS condition between each tuple (i, j) of CAVs in the network over the prediction time window T_p . The LoS condition classification from 3GPP standards depends on the obstacle type; therefore, the link between the two CAVs can be classified as NLoSb/NLoSf in the case of building or foliage blockage, NLoSv in case of vehicle blockage, and as LoS if no blockage is affecting the link.

Remark 1. Each CAV that measures the state of a k th object needs to estimate its spatial footprint. For a non-connected autonomous vehicle (nCAV), its localization of the point $(\tilde{x}_i^k(t_0), \tilde{y}_i^k(t_0))$ has an intrinsic uncertainty within the vehicle's shape. The uncertainty compounds the normal distribution of an estimate point [41] and the vehicle's shape. The result can be approximated to a normal bivariate for high uncertainty. Thus, the footprint area of the vehicle can be modelled by an isotropic disc of radius $\sigma_i^k(t_0)$, whose value is taken into account in the initialization of the covariance matrix $\tilde{\Sigma}_i^k(t_0) = \sigma_i^k(t_0)^2 \mathbf{I}$. These considerations allow us to adopt Gaussian models.

C. Prediction of the LoS-map

The cooperative sensing information collected makes it possible to predict the state of CAVs in the time window T_p . Many prediction strategies are discussed in literature [34, 42, 43, 44].

The proposed method revises and reshapes the work in [34], where the predicted state at time instant \bar{t} is

$$\tilde{\mathbf{s}}^k(\bar{t}) = \mathbf{T}(\bar{t})\tilde{\mathbf{s}}^k(t_0) + \mathbf{w}^k(\bar{t}), \quad (4)$$

where

$$\mathbf{T}(\bar{t}) = \begin{bmatrix} \mathbf{I}_2 & \bar{t} \mathbf{I}_2 \\ \mathbf{0}_{2 \times 2} & \mathbf{I}_2 \end{bmatrix} \quad (5)$$

is the transition matrix of the constant velocity model and $\mathbf{w}^k(\bar{t}) \sim \mathcal{N}(\mathbf{0}, \mathbf{Q}^k(\bar{t}))$ is the prediction error, characterized by the covariance $\mathbf{Q}^k(\bar{t})$, which is derived by fitting the numerical results of [34]. Note that the authors in [34] consider the constant turn rate and acceleration model, which would require the position, speed, heading, turn rate, and acceleration, hence, it is more complex and it requires more parameters compared to the used model.

The proposed framework, depicted in Fig. 2, exploits the predicted states to evaluate the dynamic evolution of LoS conditions among CAVs over the time window T_p .

D. Network Metrics Evaluation

The QoS of the link $i - j$ can be characterized by its SNR $\gamma^{(i,j)}(t)$. For simplicity of notation, the indexes (i, j) that identify a certain link will be omitted since the discussion can be generalized for any tuple of CAVs. The time evolution of the SNR γ depends on configurable parameters (such as transmission power and antenna gains) and non-configurable ones (such as the distance between transmitting and receiving CAVs and blocking obstacles). Static obstacles are inferred from the digital map and CA signalling, while the state of dynamic nCAVs is predicted in (4). The predicted motions make the LoS-map dynamically evolving over time (see Fig. 2).

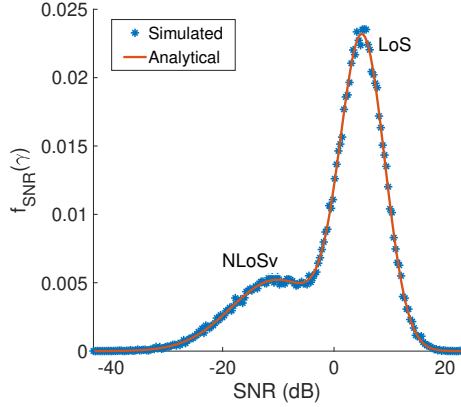
We assume that CAVs are equipped with $N_a = N_v \times N_c$ cylindrical antenna arrays on their rooftop, where N_v is the number of uniform circular arrays, characterized by N_c uniformly spaced antenna elements each as defined in [47] (any other array configuration can be used and it needs a straightforward adaptation). The SNR at time \bar{t} in decibel scale is

$$\begin{aligned} \gamma(\bar{t}) &= P_{Tx} + 2G_b - PL(\bar{t}) - P_n = \\ &= \gamma_0(\bar{t}) - PL(\bar{t}) \quad [\text{dB}] \end{aligned} \quad (6)$$

where P_{Tx} is the transmitted power, G_b is the antenna gain, P_n is the noise power, and path-loss $PL(\bar{t}) \sim \mathcal{N}(A_{LOS}(d(\bar{t})), \sigma_{sh}^2)$ contains log-normal shadowing with

Table I: Direct component characterization of the path-loss models from 3GPP [38, 45, 46]

Condition	Mean value ($A_{PL}(d)$) [dB]	Symbol	Description
LoS (highway)	$32.4 + 20 \log_{10}(d) + 20 \log_{10}(f)$	$A_{LoS}(d)$	clear link visibility
LoS (urban)	$38.77 + 16.7 \log_{10}(d) + 18.2 \log_{10}(f)$		
NLoSb	$36.85 + 30 \log_{10}(d) + 18.9 \log_{10}(f)$	$A_{NLoSb}(d)$	buildings blockage
NLoSf	$A_{LoS}(d) + A_f$	$A_{NLoSf}(d)$	foliage obstructions
NLoSv	$A_{LoS}(d) + A_v$	$A_{NLoSv}(d)$	vehicular blockage

Figure 3: Analytical and numerical SNR γ pdf

variance σ_{sh}^2 and $A_{LoS}(d(\hat{t}))$, where d refers to the distance, in Table I. The proper PL model is selected based on the 3GPP recommendations in [5, 38] given the current propagation environment, i.e., urban, rural, or highway. CAVs have access to their position and map information that are combined to obtain context information about the current propagation environment. The randomness of the SNR is analyzed next.

Remark 2. In the case of multiple blockages, the order of relevance in the $PL(\hat{t})$ computation depends on the blocker with the highest attenuation [38, 48], in order (from Table I): NLoSb, NLoSf, and lastly NLoSv. For example, if the LoS is blocked by a building and a vehicle, the used path-loss model is NLoSb.

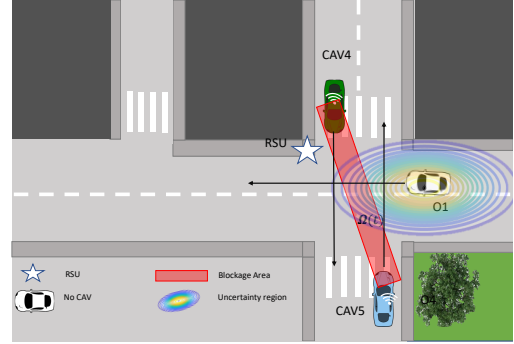
E. Link SNR Statistics

In our framework, current and future positions of all CAVs are considered known with negligible error. This assumption is based on the localization and tracking systems of self-driving CAVs that combine multiple sensors to reach sub-metre position accuracy, including the individual footprints with exact shapes [49, 50]. Furthermore, self-driving cars know their future trajectory as it is typically self planned [51]. The SNR γ distribution, based on the LoS condition, is mainly affected by the uncertainty of the nCAVs positions and shadowing.

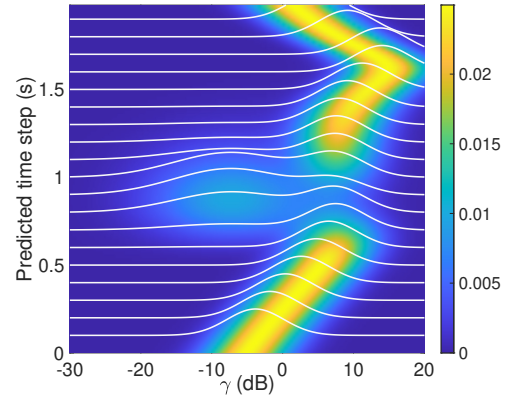
In the remaining section, we evaluate the pdf of the SNR in closed form. Two illustrative cases are considered below for the dynamic LoS-map:

- **absence of nCAVs:** the SNR distribution (in decibel scale) $f_{SNR}(\gamma)$ for the LoS and NLoSb/f cases is

$$f_{SNR}(\gamma) = \mathcal{N}(\gamma_0 - A_{PL}(d), \sigma_{sh}^2), \quad (7)$$



(a) Scenario of uncertainty between LoS and NLoSv



(b) SNR pdf versus prediction time

Figure 4: CAVs link pair SNR pdf evolution according to the predicted positions in case of uncertainty between LoS and NLoSv.

with the variance σ_{sh}^2 related to the shadowing. In case of LoS and NLoSb the term $A_{PL}(d)$ is reported in Tab. I, while for NLoSf, the path-loss PL in (6) contains an additive random term $X_{extra} \sim \mathcal{N}(A_f, \sigma_f^2)$. The extra attenuation due to the foliage A_f is computed using the concept of mean excess loss derived in [46] and the overall path-loss distribution results in $PL \sim \mathcal{N}(A_{LoS}(d) + A_f, \sigma_f^2 + \sigma_{sh}^2)$.

- **presence of nCAVs:** the SNR distribution $f_{SNR}(\gamma)$ depends on the shadowing component and the probability of blockage due to nCAVs. The extra attenuation for vehicular blockage A_v depends on the number of blocking vehicles [38]. The path-loss distribution is evaluated similarly to NLoSf case. The SNR pdf $f_{SNR}(\gamma)$ can be computed as

$$f_{SNR}(\gamma) = P_{LoS} f_{LoS}(\gamma) + \sum_{k_b=1}^{N_b} P_{NLoSv}^{(k_b)} f_{NLoSv}^{(k_b)}(\gamma), \quad (8)$$

where the term P_{LoS} is the probability of LoS condition, $f_{LoS}(\gamma)$ is the related SNR pdf, $P_{NLoSv}^{(k_b)}$ is the probability of having k_b nCAVs blockers out of N_b nCAVs, and $f_{NLoSv}^{(k_b)}(\gamma)$ is the related SNR pdf. The pdf in (8) is a mixture of Gaussians. P_{LoS} and $P_{NLoSv}^{(k_b)}$ are complementary: $P_{LoS} + \sum_{k_b=1}^{N_b} P_{NLoSv}^{(k_b)} = 1$. Their analytical derivation, together with the LoS and NLoSv SNR pdfs, are given in Appendix A. Figure 3 shows the analytical and simulated behaviour of the SNR pdf in (8) for single blockage, i.e., $k_b = N_b = 1$.

Figure 4a illustrates a realistic use case where the link between two CAVs can be obstructed by an nCAV (O1). Its SNR distribution varies according to the vehicles' relative motion directions (black arrows). The pdf of the SNR for every prediction time instant \bar{t} is reported in Fig. 4bb. It can be seen that, as soon as the nCAV uncertainty region is expected to intersect the blockage area (red polygon), the SNR drops as shown by the slices at $t \in (0.6, 1.2)$ s, and after the nCAV departure the SNR rises again.

III. PREDICTED NETWORK CONNECTIVITY

Once the SNR distribution of each link associated with the LoS-map has been predicted, the adjacency matrix of CAVs' network is used to compute the connectivity. The entries of the adjacency matrix (say links $i-j$) are defined by the probability that SNR $\gamma^{(i,j)}(t)$ is higher than a threshold γ_{th} , which is given by the minimum QoS according to the specific V2X service. The adjacency matrix is then used as input of the relay selection strategies.

A. Network Adjacency Matrix

The predicted pdfs of SNR $\gamma^{(i,j)}(t)$ are used to derive the adjacency matrix $\mathbf{A}(t) \in \mathbb{R}^{N_c \times N_c}$ of the CAVs' network in Fig 2. The entries of the matrix $\mathbf{A}(t)$ are the service probabilities that evolve with the LoS-map (or equivalently, with the motion of the vehicles):

$$[\mathbf{A}]_{(i,j)}(t) = \Pr\{\gamma^{(i,j)}(t) > \gamma_{th}\} = F_{SNR^{i,j}}(\gamma_{th}), \quad (9)$$

with $i, j = 1, \dots, N_c$ and $i \neq j$, and the cdf of the SNR $F_{SNR}(\gamma_{th})$ follows from (8), as derived in Appendix A. The network performance for link-selection, as described in Sec. IV, is based on the service probabilities in (9) over the communication interval $(t_0, t_0 + T_p]$, which is in turn discretized with sampling interval T_s . Averaging the service probabilities (9) over $N_s = T_p/T_s$ samples of the prediction window, we obtain the average *link availability* that is

$$[\bar{\mathbf{A}}]_{(i,j)} = \frac{1}{N_s} \sum_{n=0}^{N_s-1} [\mathbf{A}]_{(i,j)}(t_0 + nT_s). \quad (10)$$

The matrix of the link availabilities $\bar{\mathbf{A}}$ is symmetrical, and it is the key metric for the relay selection problem (see Secs. IV and V).

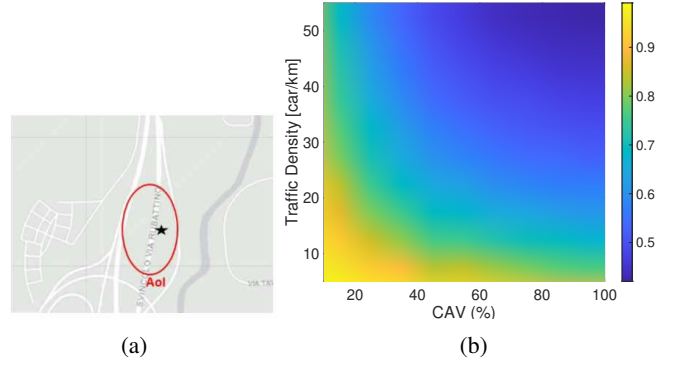


Figure 5: (a) Simulated highway scenario and (b) numerical first order network connectivity versus CAV percentage ρ_c in percentage for different traffic density condition.

B. Connectivity Analysis

The network connectivity is a metric to evaluate any need for relay nodes. Let the metric $\alpha(\bar{\mathbf{A}})$ be the measure of the connectivity of the network, $\alpha(\bar{\mathbf{A}})$ is related to the density of nCAVs and determines a-priori the reliability of the vehicles configuration and mesh of CAVs connectivity. The connectivity can be evaluated by calculating the Laplacian matrix [52]

$$\Delta \stackrel{def}{=} \mathbf{D} - \bar{\mathbf{A}}, \quad (11)$$

where the elements of \mathbf{D} are the vertex outdegrees

$$[\mathbf{D}]_{(i,i)} = \sum_{j \neq i} [\bar{\mathbf{A}}]_{(i,j)}. \quad (12)$$

The second smallest eigenvalue λ_2 of Δ defines the network connectivity $\alpha(\bar{\mathbf{A}}) = \lambda_2$, which is $\alpha(\bar{\mathbf{A}}) > 0$ in case of connected network. The second-order connectivity determines the network's robustness by considering two-hop links connecting two vehicles without any constraints on the relaying capabilities. It is obtained by substituting $\bar{\mathbf{A}}$ with $\bar{\mathbf{A}}_2$ in (11), that is defined as

$$\bar{\mathbf{A}}_2 = \bar{\mathbf{A}}^2 + \bar{\mathbf{A}}. \quad (13)$$

This can be interpreted as a performance upper-bound for the relay schemes' connectivity capability.

We study the first order connectivity in the highway scenario in Fig. 5a since it is characterized by simpler topology and mobility trajectories with respect to the urban environment. The simulation is performed by varying the traffic density and the percentage of CAV with $\gamma_{th} = 10$ dB. The V2X network based only on direct links lacks of robustness when the traffic density (veh/km) grows and for high percentage of CAVs (Fig. 5b). This is due to the impact of dynamic blockage, outlining the need for proactive relay selection strategies. These considerations are also eligible for intersection and roundabout scenarios, where relaying schemes are more needful because of the harsher propagation conditions.

C. Relay Selection

The relay selection task can be formulated as an assignment problem, which belongs to a class of optimization problems.

The goal is to maximize the network connectivity by assigning relays to RVs/VoIs based on the average availability under the constraint of limited relaying resources. In this regard, the relay selection task can be expressed as

$$\max_{\mathbf{x}} \sum_l \sum_r [\hat{\mathbf{A}}_2]_{(l,r)} [\mathbf{X}]_{l,r} \quad (14a)$$

$$\text{such that } \sum_l [\mathbf{X}]_{l,r} \leq R_c^r \quad \forall r \quad (14b)$$

$$\sum_r [\mathbf{X}]_{l,r} \leq 1 \quad \forall l, \quad (14c)$$

where l refers to the link between the i th RV and the j th VoI, r is the relay index, and $[\hat{\mathbf{A}}_2]_{(l,r)} = [\bar{\mathbf{A}}]_{(i,r)} [\bar{\mathbf{A}}]_{(j,r)}$ is the average availability of the relayed link. The assignment variable $[\mathbf{X}]_{l,r}$ is

$$[\mathbf{X}]_{l,r} = \begin{cases} 1, & \text{if } r \text{ is assigned to } l, \\ 0, & \text{otherwise.} \end{cases} \quad (15)$$

The problem in (14a) can be solved through centralized or distributed approach, as proposed below.

IV. PREDICTIVE CENTRALIZED APPROACH

Centralized link selection strategies require overall knowledge of the network state to address the following issues: *which CAVs request a link? Which CAVs are available to act as relay nodes? How CAVs are connected in the network?* Typically, a CB, such as an elected CAV, the base station, or the RSU, through periodical FR1 communications, is responsible for (i) collecting the network information, link requests, and relaying capabilities, (ii) applying the selection algorithm and (iii) communicating the decision to the involved communication parties. In this section, we first introduce the communications signalling required for information gathering and distribution of decisions. Later, we discuss the proposed algorithms for link selection.

A. Centralized Protocol

Figure 6 depicts an example time flow for the centralized protocol, i.e., the messages and procedures supporting link selection. In particular:

1) **Cooperative Sensing:** the i th CAV, after the sensing operation, obtains a list of sensed objects \mathcal{L}_i that is sent to the CB together with the CAV relaying capability R_C^i , which represents the maximum number of links it can support as a relay.

2) **Dynamic Objects Prediction:** the CB, after combining the received lists \mathcal{L}_i for each k th object (e.g., pedestrian, CAV, and nCAV), predicts the dynamic evolution of the sensed nearby objects over a predefined time window T_p , as discussed Sec. II-C.

3) **Network Metric Evaluation:** CB evaluates, for each predicted time step \bar{t} , the $\gamma^{(i,j)}(\bar{t})$ between each tuple (i, j) of CAVs in the network. The $\gamma^{(i,j)}(\bar{t})$ is computed using (6).

4) **Prediction of Dynamic Adjacency Matrix** is derived by the CB based on the previously estimated SNRs. The entries of the adjacency matrix are computed based on (9).

5) **Link Selection:** CAVs (i.e., RVs) that plan to cross an AoI could send a request for extended sensing to the CB, as depicted in Fig. 6. The CB collects the received requests and provides the optimal link based on the predicted link availability in (10) and on the link selection algorithm. If this link exists, the CB sends an acknowledgment (ACK) to the RV (otherwise, it sends a NACK), a request to the CAV supporting extended sensing, and a relay reservation request. Finally, the CB sends the necessary information to establish an FR2 communication link to the involved parties, as in Fig. 6.

The centralized protocol is executed periodically so that the information obtained through cooperative sensing is updated, and, consequently, the network metrics and the predicted link availability.

B. Centralized Link Selection

The optimization problem in (14a) is linear and, therefore, convex. There are several methods in the literature to solve it, and they differ mainly in complexity. For the centralized scheme, we consider the following approaches:

- **Exhaustive search (ES):** is the most intuitive method of finding an optimal assignment, which is achieved by searching all the possible arrangements. Considering N RVs and M relays, each with R_c^r resources, the complexity of the ES method is $\mathcal{O}((MR_c^r)^N)$.
- **Hungarian Game (HG):** is a combinatorial optimization algorithm that solves the assignment problem with polynomial time [53]. To apply the HG algorithm, we need to reformulate the assignment problem in (14a) in matrix form:

$$\min_{\mathbf{L}, \mathbf{R}} \mathbf{L} \mathbf{C} \mathbf{R} \quad (16)$$

where \mathbf{L}, \mathbf{R} are permutation matrices and $\mathbf{C} \in \mathbb{R}^{N \times MR_c^r}$ is a matrix whose elements are defined as

$$\mathbf{C} = -\hat{\mathbf{A}}_2. \quad (17)$$

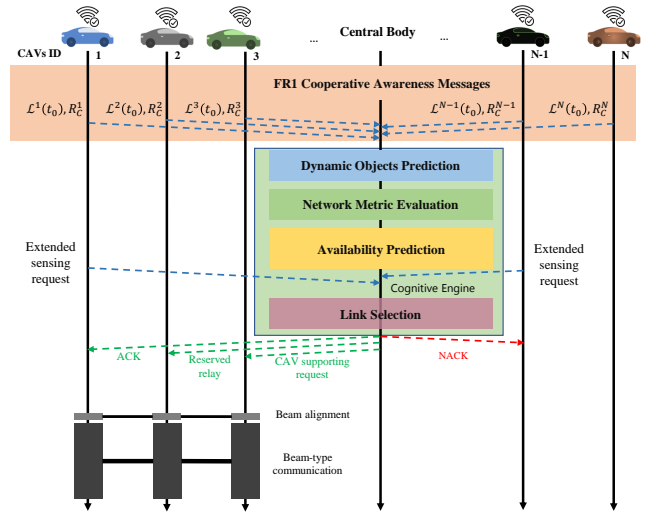


Figure 6: Centralized approach time flow example. CAVs ID1 and IDN-1 are RVs, ID3 is a VoI, and ID2 is a relay. Dashed lines are FR1 communication links, while continuous lines represent beam-type communication, e.g. FR2.

The complexity of the HG algorithm has been investigated in [54], and it is $\mathcal{O}([\min(N, MR_c^r)|C|])$. For a dense urban scenario we usually have $N \geq MR_c^r$. Therefore, the computational complexity can be expressed as $\mathcal{O}(N^2 MR_c^r)$.

V. PREDICTIVE DISTRIBUTED APPROACH

Distributed link selection approaches do not rely on a CB. CAVs individually compute the optimal link locally and compete for the available relays.

A. Distributed Protocol

The time flow of the proposed distributed architecture (Fig. 7) is similar to the centralized one. The main differences are related to cooperative sensing and link selection that are executed locally by the RVs only. In particular:

1) **Cooperative sensing:** differently from the centralized method, each CAV shares with neighbouring CAVs the list of detected objects \mathcal{L}_i and its relaying capability R_C^i .

2) **Link selection and resources reservation:** each RV executes the link selection algorithm based on the predicted link availabilities in (10). The RVs send resources reservations requests to the selected relays, as depicted in Fig. 7. The relays, based on their available relaying capabilities, reply to the RVs with positive or negative feedbacks.

As for the centralized case, the distributed protocol is executed periodically to update the cooperative sensing information and the predicted link availability.

B. Distributed Link Selection

The optimization problem in (14a) regarding the maximization of the network connectivity is here solved in a distributed manner. Two distributed algorithms are detailed below:

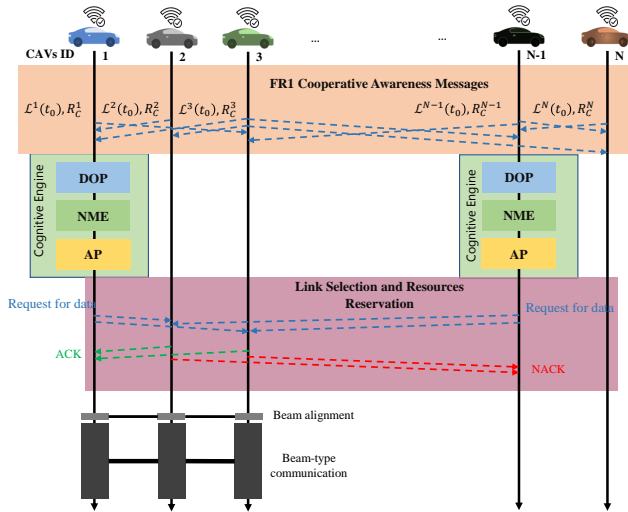


Figure 7: Distributed approach time flow example. CAVs ID1 and IDN-1 are RVs, ID3 is a VoI, and ID2 is a relay. Dashed lines are FR1 communication links, while continuous lines represents beam-type communication, e.g., FR2.

• **First Come First Served (FCFS):** is based on the *first input first output* scheduling strategy. The RV sends the request for resource reservation to the r th relay associated to the maximum link availability $[\hat{A}_2]_{(l,r)}$. If the relay's capability is sufficient, it sends a ACK, otherwise a NACK. The relays are assigned sequentially, therefore, computational complexity is $\mathcal{O}(M)$.

• **Alternating Direction Method of Multipliers (ADMM):** solves a global optimization problem by splitting it into smaller local subproblems, which iteratively attempt to find the optimal global solution [55]. Using ADMM involves creating copies of the optimization variables that are shared by different RVs. The optimization problem in (14a) can be reformulated as

$$\min_{\mathbf{x}} \sum_l \mathbf{x}_l \mathbf{c}_l^T \quad (18a)$$

$$\text{such that } \sum_l \mathbf{x}_l \leq R_c^r \mathbf{1}_M \quad (18b)$$

$$\mathbf{x}_l \mathbf{1}_M \leq 1 \quad \forall l, \quad (18c)$$

where the optimization variable is $\mathbf{x}_l \in \mathbb{R}^{1 \times M}$ is the l th row of the selection matrix \mathbf{X} in (14a), $\mathbf{c}_l \in \mathbb{R}^{1 \times M}$ is the l th row of the matrix \mathbf{C} in (17). The ADMM algorithm solves the problem in (18a) iteratively using the method of Lagrangian multiplier [55].

Example: To make an exemplary case and to clarify the ADMM application, let us assume $N = 2$. The optimization problem in (18a) simplifies to

$$\min_{\mathbf{x}_1, \mathbf{x}_2} f(\mathbf{x}_1) + f(\mathbf{x}_2) \quad (19a)$$

$$\text{such that } \mathbf{x}_1 + \mathbf{x}_2 \leq R_c^r \mathbf{1}_M \quad (19b)$$

$$\mathbf{x}_1 \mathbf{1}_M \leq 1 \quad (19c)$$

$$\mathbf{x}_2 \mathbf{1}_M \leq 1, \quad (19d)$$

where the objective function $f(\mathbf{x}) = \mathbf{x} \mathbf{c}^T$ makes the optimization convex. The augmented Lagrangian incorporates the constraints (19b),(19c),(19d):

$$\begin{aligned} L_\rho(\mathbf{x}_1, \mathbf{x}_2, \mathbf{v}_1, \mathbf{v}_2, \mathbf{v}_3) &= f(\mathbf{x}_1) + f(\mathbf{x}_2) \\ &+ \mathbf{v}_1^T (\mathbf{x}_1 + \mathbf{x}_2 - R_c^r \mathbf{1}_M) + \mathbf{v}_2^T (\mathbf{x}_1 \mathbf{1}_M - 1) \\ &+ \mathbf{v}_3^T (\mathbf{x}_2 \mathbf{1}_M - 1) + \frac{\rho}{2} \|\mathbf{x}_1 + \mathbf{x}_2 - R_c^r \mathbf{1}_M\|_2^2 \\ &+ \frac{\rho}{2} \|\mathbf{x}_1 \mathbf{1}_M - 1\|_2^2 + \frac{\rho}{2} \|\mathbf{x}_2 \mathbf{1}_M - 1\|_2^2, \end{aligned} \quad (20)$$

The optimization variables \mathbf{x}_1 and \mathbf{x}_2 are updated

$$\mathbf{x}_1^{(k+1)} := \min_{\mathbf{x}_1} L_\rho(\mathbf{x}_1, \mathbf{x}_2^{(k)}, \mathbf{v}_1^{(k)}, \mathbf{v}_2^{(k)}), \quad (21a)$$

$$\mathbf{x}_2^{(k+1)} := \min_{\mathbf{x}_2} L_\rho(\mathbf{x}_1^{(k+1)}, \mathbf{x}_2, \mathbf{v}_1^{(k)}, \mathbf{v}_3^{(k)}), \quad (21b)$$

and the Lagrangian multipliers \mathbf{v}_1 , \mathbf{v}_2 , and \mathbf{v}_3 update are

$$\mathbf{v}_1^{(k+1)} := \mathbf{v}_1^{(k)} + \rho(\mathbf{x}_1^{(k+1)} + \mathbf{x}_2^{(k+1)} - R_c^r \mathbf{1}_M), \quad (22a)$$

$$\mathbf{v}_2^{(k+1)} := \mathbf{v}_2^{(k)} + \rho(\mathbf{x}_1^{(k+1)} \mathbf{1}_M - 1), \quad (22b)$$

$$\mathbf{v}_3^{(k+1)} := \mathbf{v}_3^{(k)} + \rho(\mathbf{x}_2^{(k+1)} \mathbf{1}_M - 1). \quad (22c)$$

The updated variables $\mathbf{x}_1^{(k+1)}$, $\mathbf{x}_2^{(k+1)}$, $\mathbf{v}_1^{(k+1)}$, $\mathbf{v}_2^{(k+1)}$, and $\mathbf{v}_3^{(k+1)}$ are shared among the RVs through signaling in FR1.

Table II: Summary of computational complexity

Algorithm	Complexity
Exhaustive Search	$\mathcal{O}((MR_c^r)^N)$
Hungarian Game	$\mathcal{O}(N^2 MR_c^r)$
FCFS	$\mathcal{O}(M)$
ADMM	$\mathcal{O}(T_k(NM + N + 1))$

The stopping criterion depends both on the residual convergence to zero, and on the maximum number of iterations that can be fixed. Therefore, the ADMM complexity is $\mathcal{O}(T_k(NM + N + 1))$, where T_k is the number of iterations considered, which depends on the maximum tolerable delay induced by signaling.

VI. SIMULATIONS FRAMEWORK

The mmW V2X communication is characterized by highly dynamic and sparse propagation channels [56, 57], subject to blockage by nCAVs, buildings, and trees. To better capture the system's complexity, the proposed framework combines several tools to simulate a realistic scenario, as depicted in Fig. 8. In particular, the simulation environments, i.e., road network topology, buildings, and vegetation, are obtained from OSM [35]. Realistic vehicular mobility is simulated by SUMO [36], and the GEMV² [37] software generates the wireless channel in Matlab.

This section describes how the software tools are combined and set for numerical validation. Table III reports the main parameters used for the communications by following the 3GPP recommendations in [58].

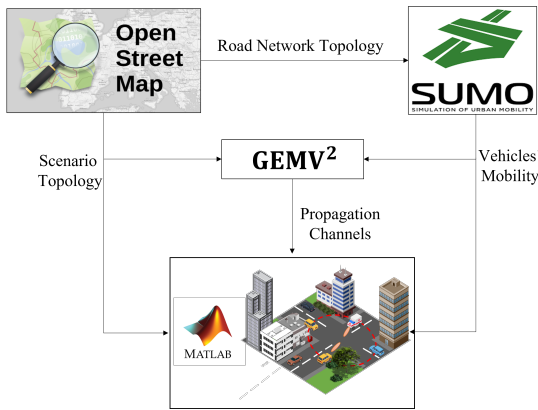


Figure 8: Simulation Methodology

Table III: Simulation parameters

Parameter	Value	Description
P_{Tx}	10 dBm	Maximum transmitted Power
P_n	-85.5 dBm	Noise power
f_c^1	5.2 GHz	FR1 carrier frequency
f_c^2	28 GHz	FR2 carrier frequency
N_a	4×16	Number of antenna elements
T_p	1 s	Predicted time window
R_c^r	2	Maximum number of relay requests granted by a CAV and RSU



(a) Intersection

(b) Roundabout

Figure 9: Simulated urban blind intersection (a) and roundabout (b).

A. Simulated Scenarios

A blind intersection (Fig. 9a) and a roundabout scenario (Fig. 9b) are deemed to evaluate the performances of the proposed relay selection schemes. The selected areas are located around the city of Milan, Italy. For each scenario, the AoI represents the critical area in the road environment. The CAVs, whose sensors' field of view is within the AoI are the VoIs. The range of the AoI (red circle) in the intersection and roundabout is 70 m and 90 m, respectively, and depends on the road patterns. The RSUs are deployed in strategic positions, e.g., in the centre of the roundabout (see Fig. 9), to assist the communication.

B. Vehicles Topology and Mobility

Simulation of vehicles' mobility is performed by SUMO software that allows for realistic traffic data generation. The *road network*, used as input to SUMO, is generated from the selected OSM scenario. The output is processed in MATLAB together with the OSM scenario. Two vehicular density are simulated: medium and high with an average of 50 veh/km and 70 veh/km, respectively.

C. V2X Communications Channel

GEMV² [37] is an open-source solution for V2X channel modelling with good accuracy and low complexity. It evaluates geometrically the propagation conditions and reflections using the outlines of buildings and foliage, provided by OSM, and the vehicles' ones, provided by SUMO. The propagation parameters used in the considered scenarios are defined according to the recommendations of 3GPP and International Telecommunications Union (ITU). In particular, we select the relative permittivity of ground, buildings, and vehicles based on the ITU measurements in [59]. The PL models for the propagation conditions are defined in Table I. GEMV² outputs the space-time features of the propagation channel, i.e., small and large scale channel components, delays, angles of departure, and angles of arrivals, which are used in (6) to evaluate the SNR for each link pair.

VII. NUMERICAL RESULTS

This section shows and discusses the numerical results obtained for the proactive relaying schemes, above described, in terms of network connectivity and computational complexity.

The performance of the proactive relay of opportunity selection approaches, which leverage on the proposed LoS-map prediction, is here compared with the analytical network connectivity bounds. The lower bound, which accounts only for the direct links, is analytically derived based on the average adjacency matrix $\bar{\mathbf{A}}$ according to the real channel state. The upper bound is the ideal case where *all* the nodes of the V2X network can act as relays with unlimited resource capabilities. This is obtained by evaluating the second-order average adjacency matrix $\bar{\mathbf{A}}_2$, as defined in (13). Once the lower and upper bound are defined, a good relaying strategy is expected to attain the upper bound, even if it is limited by relaying resource capabilities R_c^r and it is affected by the uncertainty on the SNR link characterization.

The output of the relay selection algorithms is the adjacency matrix $\bar{\mathbf{A}}_R$, whose entry $[\bar{\mathbf{A}}_R]_{(i,j)} = [\bar{\mathbf{A}}]_{(i,j)}$ if a relay has been successfully allocated, as in (10). The network

connectivity is obtained as in (11) by replacing $\bar{\mathbf{A}}$ with $\bar{\mathbf{A}}_R$.

The network connectivity versus the SNR threshold γ_{th} is evaluated for the intersection in Fig. 10 and the roundabout in Fig. 11 for two different traffic densities in the case of 100% of CAVs. The average network connectivity in the roundabout scenario is higher than the intersection one, since CAVs are in LoS condition with high probability. Generally, in the intersection scenario, the network connectivity upper bound is significantly below 1. This is due to the strong attenuation from blocking buildings, which severely limits the visibility of the CAVs. The increase of vehicular density determines a more recurrent dynamic blockage of CAVs, thus leading to the degradation of the network connectivity bounds, as can be noticed by comparing scenarios with medium traffic density in Fig. 10a and 11a and high traffic density in Fig. 10b and 11b. The proactive relay selection schemes counteract the blockage from CAVs by guaranteeing high network connectivity that

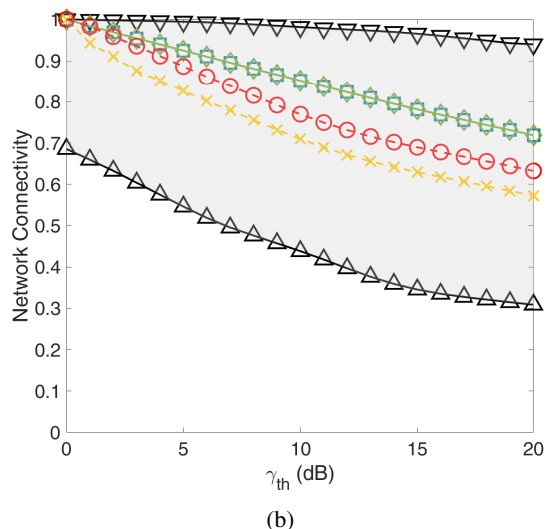
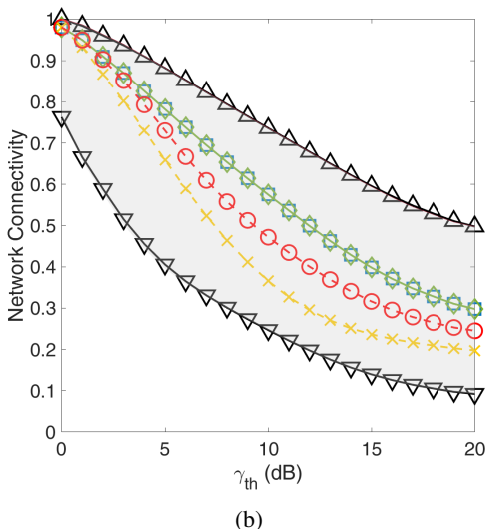
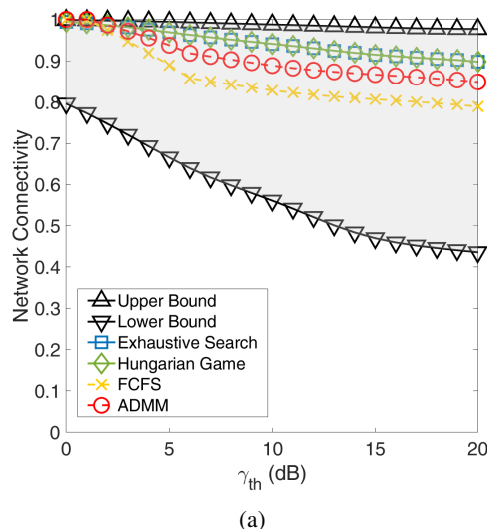
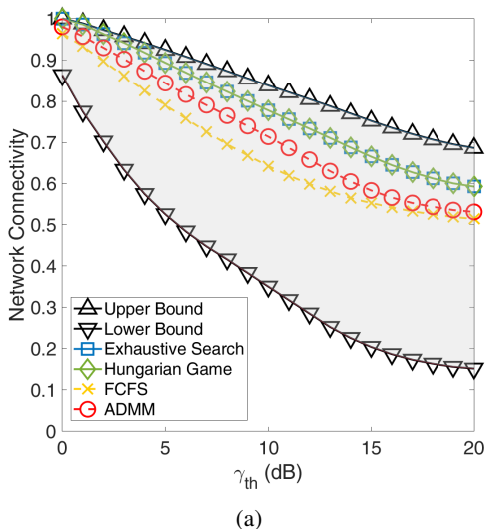
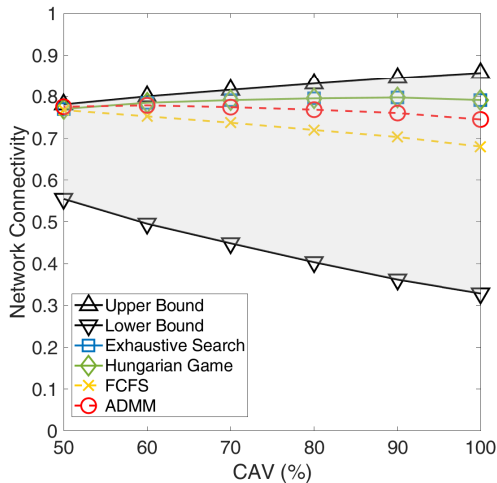
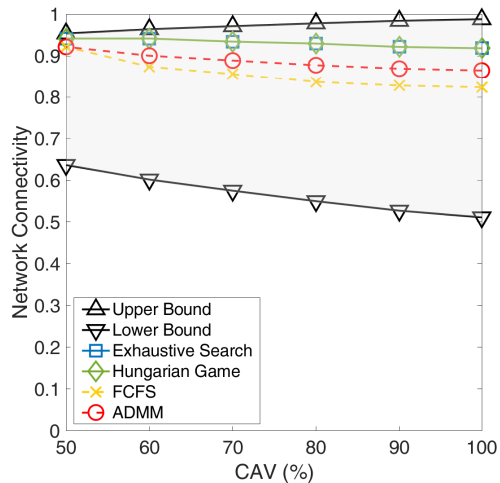


Figure 10: Network connectivity versus SNR γ_{th} in urban intersection: (a) medium and (b) high vehicular density for all CAVs.

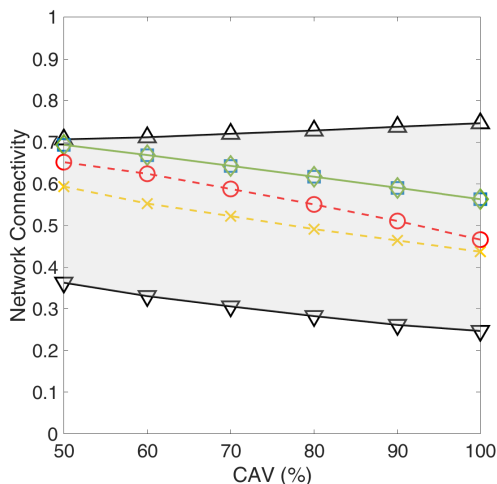
Figure 11: Network connectivity versus SNR γ_{th} in urban roundabout: (a) medium and (b) high vehicular density for all CAVs.



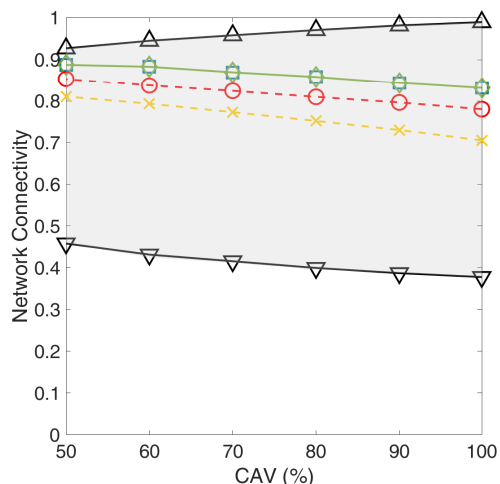
(a)



(a)



(b)



(b)

Figure 12: Network connectivity versus CAV percentage in urban intersection: (a) medium and (b) high vehicular density.

Figure 13: Network connectivity versus CAV percentage in urban roundabout: (a) medium and (b) high vehicular density.

attains the upper bound. The proactive centralized approaches (ES and HG) always coincide and outperform the distributed ones, whose local decisions may lead to collisions and average network connectivity decrease. Centralized schemes are more robust in high traffic density compared to distributed techniques, but requiring more V2I signalling.

Figures 12 and 13 depict the V2X network connectivity varying the density of CAVs given the SNR threshold $\gamma_{th} = 10$ dB. As the percentage of CAVs increases, the lower bound decreases due to the high impact of recurring dynamic blockage. By contrast, the upper bound improves due to the high relaying resource capabilities, leading to a higher probability of connecting two nodes with relayed links that satisfy the SNR requirements. However, the performance of the relay selection strategies decreases as the CAVs percentage increases. This behavior is induced by the limited relay resources, suggesting that future CAVs need to support a higher communication overhead and have to increase resources for opportunistic

relaying operations. The effect of the random blockage due to nCAVs is observed at medium and high traffic densities in Figs. 12a, 13a and Figs. 12b, 13b for a fixed CAV percentage. The proposed proactive relay selection strategies prove to counteract the effect of the probabilistic blockage of nCAVs as they achieve an average network connectivity comparable to the upper bound, when the percentage of CAVs is around 50-70%.

The proactive distributed relay selection schemes are preferred in case of low percentage of CAVs and low γ_{th} as they achieve stable network connectivity with a limited computational complexity, as described in Table II. The centralized approaches are suggested in case of high CAVs density and high SNR threshold since they achieve high connectivity and they are more robust in counteracting dynamic blockage, but they require an higher computational cost.

Results here highlight the strong need to develop proactive robust and resilient relaying techniques that optimizes the

network connectivity during the communication interval. Our work provides an innovative relaying framework to guarantee the SNR QoS requirements over the communication interval that maximizes the average probability of connecting nodes with reliable links.

VIII. CONCLUSION

Millimeter-wave (mmW) multiple-input multiple-output (MIMO) technology, using beamforming, is expected to support enhanced vehicle-to-everything (V2X) services. Link quality degrades severely at high frequencies, considering that the mobility of vehicles causes frequent blockage of the line-of-sight (LoS). Traditional relaying techniques implement a reactive scheme to link failure and leverage only with instantaneous information, which impedes efficient relay selection in highly mobile and complex networks, such as vehicular scenarios. In this paper, a unified framework for proactive relay selection is proposed as a tool to mitigate blockage in vehicular networks. In particular, a novel architecture for proactive relay of opportunity selection in 6G V2X is investigated. Here, the reliable lower spectrum (FR1) link enables the signaling to exchange the cooperative awareness messages and periodic position information. Based on this collected information and onboard sensors, connected and autonomous vehicles (CAVs) estimate the state of nearby objects to predict the dynamic LoS-map, which describes the network links' evolution in time. The proactive relaying schemes exploit the dynamic LoS-map to maximize the network connectivity. Centralized and distributed architectures are considered and compared in terms of network connectivity and complexity. Moreover, the upper and lower bounds of the network connectivity are derived analytically and are used to compare different relaying methods. The proposed framework and the analytical tools are validated through numerical simulations in realistic scenarios and different traffic densities. The results suggest that LoS blockage has a severe impact on communication in 6G vehicular networks. Further, the proactive relay-based solutions are required to mitigate blockage and maximize the average probability of connecting CAVs with reliable links.

APPENDIX A

This section presents the analytical derivation of the SNR distribution. The absence of nCAVs and the assumption of knowing the positions of the VoI and RV, as well as the objects' (e.g., buildings, foliage, and other CAVs) footprint, make the SNR pdf solely dependent on the shadowing component. On the contrary, if nCAVs are part of the considered scenario determining the NLoSv condition (see Remark 2), the SNR pdf also depends on the probability that a single nCAV (or several nCAVs) block(s)the LoS. Therefore, to analytically derive the distribution of the SNR, it is necessary to obtain this probability.

A. Single nCAV Blockage

For sake of simplicity, we first consider the case of a single nCAV, whose state $\tilde{\mathbf{s}}$ at time instant \tilde{t} (hereinafter omitted for clarity of notation) is modeled as in Sec. II-B. To

derive the blockage probability, we consider only the position information $\tilde{\mathbf{s}}_p = [\tilde{x}, \tilde{y}]$, that is

$$\tilde{\mathbf{s}}_p \sim \mathcal{N}(\mathbf{s}_{p,\text{true}}, \tilde{\Sigma}_p), \quad (26)$$

where $\tilde{\Sigma}_p$ is defined in (3). The blockage probability P_{NLoSv} is given in (23), where Ω represents the blockage area (see Fig. 4a). The double integral in (23) admits a closed form solution if the blockage area $\Omega \approx [x_1, x_2] \times [y_1, y_2]$ is approximately rectangular and the covariance matrix $\tilde{\Sigma}_p = \text{diag}(\sigma_x^2, \sigma_y^2)$ is diagonal. In this case, the probability of blockage P_{NLoSv} is obtained in (24), where $\mathcal{Q}(\cdot)$ is the Q-function. The LoS probability is obtained by $P_{LoS} = 1 - P_{NLoSv}$. The SNR distribution $f_{\text{SNR}}(\gamma)$ is computed in (25) as a mixture of two normal distributions, which represent the two concurring propagation conditions (LoS and NLoSv). An example of (25) is depicted in Fig. 3. To derive the service probability in (9), we evaluate the cdf of the SNR as

$$F_{\text{SNR}}(\gamma_{\text{th}}) = P_{LoS}F_{LoS}(\gamma_{\text{th}}) + P_{NLoSv}F_{NLoSv}(\gamma_{\text{th}}) \quad (27)$$

where $F_{LoS}(\gamma_{\text{th}})$ and $F_{NLoSv}(\gamma_{\text{th}})$ are the cdfs of LoS and NLoS conditions, respectively. The cdf of a normal distribution $x \sim \mathcal{N}(\mu, \sigma^2)$ can be computed as

$$F_X(x) = 1 - \mathcal{Q}(x) \quad (28)$$

B. Multiple nCAVs Blockage

We generalize the blockage probability derivation to the case of multiple blockers. Assuming the presence of N_b nCAVs, whose state position is defined in (26), the SNR distribution depends on the shadowing component and on the effective number k_b of nCAVs simultaneously blocking the LoS, with $1 \leq k_b \leq N_b$. This can be undertaken as a combinatorial problem. Indeed, to derive the probability $P_{NLoSv}^{(k_b)}$ that k_b out of N_b nCAVs are blocking the LoS, evaluation of all possible combinations is required. The total number of combinations is given by the binomial coefficient

$$N(k_b) = \binom{N_b}{k_b} = \frac{N_b!}{(N_b - k_b)!k_b!}. \quad (29)$$

We refer to the single n th k_b -tuple as \mathbf{b}_n , with $1 \leq n \leq N(k_b)$. The NLoSv probability due to k_b nCAVs effective blockers is

$$P_{NLoSv}^{(k_b)} = \sum_{n=1}^{N(k_b)} \left(\prod_{i \in \mathbf{b}_n} P_{NLoSv}^{(i)} \prod_{\substack{j \notin \mathbf{b}_n \\ j \in [1, N_b]}} (1 - P_{NLoSv}^{(j)}) \right). \quad (30)$$

For example, if we consider $N_b = 3$ nCAVs with index $i = \{1, 2, 3\}$, the probability that $k_b = 2$ of them block the LoS according to (30) is

$$P_{NLoSv}^{(2)} = p^{(1)}p^{(2)}(1 - p^{(3)}) + p^{(1)}p^{(3)}(1 - p^{(2)}) + p^{(2)}p^{(3)}(1 - p^{(1)}) \quad (31)$$

where $p^{(i)}$ is the probability that the i th nCAV is blocking the LoS.

$$P_{NLoSv} = \iint_{\Omega} \frac{1}{\sqrt{2\pi \det(\tilde{\Sigma}_p)}} \exp\left(-\frac{1}{2}(\mathbf{s}_p - \mathbf{s}_{p,\text{true}})^H \tilde{\Sigma}_p^{-1} (\mathbf{s}_p - \mathbf{s}_{p,\text{true}})\right) d\Omega \quad (23)$$

$$P_{NLoSv} = \left(\mathcal{Q}\left(\frac{x_1 - x_{\text{true}}}{\sigma_x}\right) - \mathcal{Q}\left(\frac{x_2 - x_{\text{true}}}{\sigma_x}\right) \right) \left(\mathcal{Q}\left(\frac{y_1 - y_{\text{true}}}{\sigma_y}\right) - \mathcal{Q}\left(\frac{y_2 - y_{\text{true}}}{\sigma_y}\right) \right) \quad (24)$$

$$f_{\text{SNR}}(\gamma) = \underbrace{P_{LoS} \frac{1}{\sqrt{2\pi\sigma_{sh}^2}} \exp\left(-\frac{(\gamma - A_{LoS}(d))}{2(\sigma_{sh}^2)}\right)}_{\text{LoS component } f_{LoS}(\gamma)} + \underbrace{P_{NLoSv} \frac{1}{\sqrt{2\pi(\sigma_v^2 + \sigma_{sh}^2)}} \exp\left(-\frac{(\gamma - (A_{LoS}(d) + A_v))}{2(\sigma_v^2 + \sigma_{sh}^2)}\right)}_{\text{NLoSv component } f_{NLoSv}(\gamma)} \quad (25)$$

Finally, the SNR distribution $f_{\text{SNR}}(\gamma)$ is a mixture of Gaussians, computed as

$$f_{\text{SNR}}(\gamma) = P_{LoS} f_{LoS}(\gamma) + \sum_{k_b=1}^{N_b} P_{NLoSv}^{(k_b)} f_{NLoSv}^{(k_b)}(\gamma) \quad (32)$$

where $f_{NLoSv}^{(k_b)}(\gamma)$ is the SNR pdf in case of k_b blocking vehicles and $P_{LoS} = 1 - \sum_{k_b=1}^{N_b} P_{NLoSv}^{(k_b)}$. The mean $A_v^{(k_b)}$ and the variance $\sigma_v^{2(k_b)}$ of the extra attenuation depend on k_b according to the 3GPP recommendations [38]. Similarly, the cdf of the SNR in the multiple nCAVs blockage is obtained as

$$F_{\text{SNR}}(\gamma_{\text{th}}) = P_{LoS} F_L(\gamma_{\text{th}}) + \sum_{k_b=1}^{N_b} P_{NLoSv}^{(k_b)} F_{NLoSv}^{(k_b)}(\gamma_{\text{th}}) \quad (33)$$

This result is used to determine the service probability in (9).

ACKNOWLEDGMENT

This research was carried out in the framework of the Huawei-Politecnico di Milano Joint Research Lab. The Authors want to acknowledge the Huawei Milan Research Centre.

REFERENCES

- [1] Z. MacHardy, A. Khan, K. Obana, and S. Iwashina, "V2x access technologies: Regulation, research, and remaining challenges," *IEEE Communications Surveys Tutorials*, vol. 20, no. 3, pp. 1858–1877, 2018.
- [2] J. Wang, J. Liu, and N. Kato, "Networking and communications in autonomous driving: A survey," *IEEE Communications Surveys Tutorials*, vol. 21, no. 2, pp. 1243–1274, 2019.
- [3] K. Abboud, H. A. Omar, and W. Zhuang, "Interworking of dsrc and cellular network technologies for v2x communications: A survey," *IEEE Transactions on Vehicular Technology*, vol. 65, no. 12, pp. 9457–9470, 2016.
- [4] R. Molina-Masegosa, J. Gozalvez, and M. Sepulcre, "Configuration of the c-v2x mode 4 sidelink pc5 interface for vehicular communication," in *2018 14th International Conference on Mobile Ad-Hoc and Sensor Networks (MSN)*, 2018, pp. 43–48.
- [5] 3GPP TS 22.186 v16.2.0, "3rd Generation Partnership Project; technical specification group services and system aspects; study on enhancement of 3GPP support for 5G V2X services (Release 16)," Nov. 2020.
- [6] K. Sakaguchi, R. Fukatsu, T. Yu, E. Fukuda, K. Mahler, R. Heath, T. Fujii, K. Takahashi, A. Khoryaev, S. Nagata, and T. Shimizu, "Towards mmwave v2x in 5g and beyond to support automated driving," 2020.
- [7] 3GPP, "Study on enhancement of 3gpp support for 5g v2x services," 3rd Generation Partnership Project (3GPP), Tech. Rep. RP22.886, Dec. 2018.
- [8] 3rd Generation Partnership Project. (2021) 3GPP Release 17. [Online]. Available: <https://www.3gpp.org/release-17>
- [9] A. Molina-Galan, B. Coll-Perales, and J. Gozalvez, "C-v2x assisted mmwave v2v scheduling," in *2019 IEEE 2nd Connected and Automated Vehicles Symposium (CAVS)*, 2019, pp. 1–5.
- [10] S. Sun, T. S. Rappaport, M. Shafi, P. Tang, J. Zhang, and P. J. Smith, "Propagation models and performance evaluation for 5g millimeter-wave bands," *IEEE Transactions on Vehicular Technology*, vol. 67, no. 9, pp. 8422–8439, 2018.
- [11] T. S. Rappaport, S. Sun, R. Mayzus, H. Zhao, Y. Azar, K. Wang, G. N. Wong, J. K. Schulz, M. Samimi, and F. Gutierrez, "Millimeter Wave Mobile Communications for 5G Cellular: It Will Work!" *IEEE Access*, vol. 1, pp. 335–349, May 2013.
- [12] Z. Li, L. Xiang, X. Ge, G. Mao, and H.-C. Chao, "Latency and reliability of mmwave multi-hop v2v communications under relay selections," *IEEE Transactions on Vehicular Technology*, vol. 69, no. 9, pp. 9807–9821, 2020.
- [13] D. Tian, J. Zhou, Z. Sheng, M. Chen, Q. Ni, and V. C. M. Leung, "Self-organized relay selection for cooperative transmission in vehicular ad-hoc networks," *IEEE Transactions on Vehicular Technology*, vol. 66, no. 10, pp. 9534–9549, 2017.
- [14] P. Wang, J. Fang, X. Yuan, Z. Chen, and H. Li, "Intelligent reflecting surface-assisted millimeter wave communications: Joint active and passive precoding design," *IEEE Transactions on Vehicular Technology*, vol. 69, no. 12, pp. 14960–14973, 2020.
- [15] B. Gu, Y. Wei, M. Song, F. R. Yu, and Z. Han, "Auction-based relay selection and power allocation in green relay-assisted cellular networks," *IEEE Transactions on Vehicular Technology*, vol. 68, no. 8, pp. 8000–8011, 2019.
- [16] D. Lin, J. Kang, A. Squicciarini, Y. Wu, S. Gurung, and O. Tonguz, "Moza: A moving zone based routing protocol using pure v2v communication in vanets," *IEEE Transactions on Mobile Computing*, vol. 16, no. 5, pp. 1357–1370, 2017.
- [17] X. Wang, T. Jin, L. Hu, and Z. Qian, "Energy-efficient power allocation and q-learning-based relay selection for relay-aided d2d communication," *IEEE Transactions on Vehicular Technology*, vol. 69, no. 6, pp. 6452–6462, 2020.
- [18] J. Ghosh, H. Zhu, and H. Hacı, "A novel channel model and optimal beam tracking schemes for mobile millimeter-wave massive mimo communications," *IEEE Transactions on Vehicular Technology*, vol. 70, no. 7, pp. 7205–7210, 2021.
- [19] K. Eshteiwi, G. Kaddoum, K. Ben Fredj, E. Soujeri, and F. Gagnon, "Performance analysis of full-duplex vehicle relay-based selection in dense multi-lane highways," *IEEE Access*, vol. 7, pp. 61581–61595, 2019.

- [20] H. Guo, B. Makki, D.-T. Phan-Huy, E. Dahlman, M.-S. Alouini, and T. Svensson, "Predictor antenna: A technique to boost the performance of moving relays," 2021.
- [21] D. Cao, Y. Liu, X. Ma, J. Wang, B. Ji, C. Feng, and J. Si, "A relay-node selection on curve road in vehicular networks," *IEEE Access*, vol. 7, pp. 12 714–12 728, 2019.
- [22] S. Mahesh, B. A. Reddy, B. H. Reddy, K. S. Kumar, and I. Chandra, "Routing communication performance in mobile ad-hoc networks using millimeter wave-an survey," 2019.
- [23] B. Zhang, Q. Lu, C. Shi, N. Yang, B. Leng, and Z. Du, "Sidelink relay in nr and nr advanced," in *2021 IEEE/CIC International Conference on Communications in China (ICCC Workshops)*, 2021, pp. 358–362.
- [24] B. Pan and H. Wu, "Modeling and analysis of multi-relay cooperative communications in c-v2x networks," *IEEE Transactions on Intelligent Transportation Systems*, pp. 1–15, 2022.
- [25] I. Ullah, M. Z. Asghar, L. Bariah, S. Muhaidat, and J. Hämäläinen, "Performance evaluation of relaying with different relay selection schemes in 5g nr v2x communications," in *2021 4th International Conference on Advanced Communication Technologies and Networking (CommNet)*, 2021, pp. 1–7.
- [26] J. Wu, H. Lu, Y. Xiang, R. Wu, and F. Wang, "Mbr: A map-based relaying algorithm for reliable data transmission through intersection in vanets," *IEEE Transactions on Intelligent Transportation Systems*, vol. 20, no. 10, pp. 3661–3674, 2019.
- [27] B. Fan, H. Tian, S. Zhu, Y. Chen, and X. Zhu, "Traffic-aware relay vehicle selection in millimeter-wave vehicle-to-vehicle communication," *IEEE Wireless Communications Letters*, vol. 8, no. 2, pp. 400–403, 2019.
- [28] M. Mezzavilla, M. Zhang, M. Polese, R. Ford, S. Dutta, S. Rangan, and M. Zorzi, "End-to-end simulation of 5g mmwave networks," *IEEE Communications Surveys & Tutorials*, vol. 20, no. 3, pp. 2237–2263, 2018.
- [29] G. F. Riley and T. R. Henderson, "The ns-3 network simulator," in *Modeling and tools for network simulation*. Springer, 2010, pp. 15–34.
- [30] N. Patriciello, S. Lagen, B. Bojovic, and L. Giupponi, "An e2e simulator for 5g nr networks," *Simulation Modelling Practice and Theory*, vol. 96, p. 101933, 2019.
- [31] S. Wang, J. Huang, and X. Zhang, "Demystifying millimeter-wave v2x: Towards robust and efficient directional connectivity under high mobility," in *Proceedings of the 26th Annual International Conference on Mobile Computing and Networking*, 2020, pp. 1–14.
- [32] M. Lübke, H. Hamoud, J. Fuchs, A. Dubey, R. Weigel, and F. Lurz, "Channel characterization at 77 ghz for vehicular communication," in *2020 IEEE Vehicular Networking Conference (VNC)*. IEEE, 2020, pp. 1–4.
- [33] G. Thandavarayan, M. Sepulcre, and J. Gozalvez, "Cooperative perception for connected and automated vehicles: Evaluation and impact of congestion control," *IEEE Access*, vol. 8, pp. 197 665–197 683, 2020.
- [34] G. Xie, H. Gao, L. Qian, B. Huang, K. Li, and J. Wang, "Vehicle trajectory prediction by integrating physics-and maneuver-based approaches using interactive multiple models," *IEEE Transactions on Industrial Electronics*, vol. 65, no. 7, pp. 5999–6008, 2017.
- [35] OpenStreetMap contributors, "Planet dump retrieved from <https://planet.osm.org>," <https://www.openstreetmap.org>, 2017.
- [36] P. A. Lopez, M. Behrisch, L. Bieker-Walz, J. Erdmann, Y.-P. Flötteröd, R. Hilbrich, L. Lücken, J. Rummel, P. Wagner, and E. Wießner, "Microscopic traffic simulation using sumo," in *The 21st IEEE International Conference on Intelligent Transportation Systems*. IEEE, 2018. [Online]. Available: <https://elib.dlr.de/124092/>
- [37] B. Aygun, M. Boban, J. P. Vilela, and A. M. Wyglinski, "Geometry-based propagation modeling and simulation of vehicle-to-infrastructure links," in *2016 IEEE 83rd Vehicular Technology Conference (VTC Spring)*, 2016, pp. 1–5.
- [38] 3GPP, "Study on evaluation methodology of new v2x use cases for lte and nr," 3rd Generation Partnership Project (3GPP), Tech. Rep. TS37.885, 2019.
- [39] J. Choi, V. Va, N. Gonzalez-Prelcic, R. Daniels, C. R. Bhat, and R. W. Heath, "Millimeter-wave vehicular communication to support massive automotive sensing," *IEEE Commun. Mag.*, vol. 54, no. 12, pp. 160–167, 2016.
- [40] ETSI EN 302 637-2 V1.3.2, "Intelligent Transport Systems (ITS); Vehicular Communications; Basic Set of Applications; Part 2: Specification of Cooperative Awareness Basic Service," Nov. 2014.
- [41] M. Shan, K. Narula, Y. F. Wong, S. Worrall, M. Khan, P. Alexander, and E. Nebot, "Demonstrations of cooperative perception: Safety and robustness in connected and automated vehicle operations," *Sensors*, vol. 21, no. 1, 2021. [Online]. Available: <https://www.mdpi.com/1424-8220/21/1/200>
- [42] G. Soatti, M. Nicoli, N. Garcia, B. Denis, R. Raulefs, and H. Wymeersch, "Implicit cooperative positioning in vehicular networks," *IEEE Transactions on Intelligent Transportation Systems*, vol. 19, no. 12, pp. 3964–3980, 2018.
- [43] A. Houenou, P. Bonnifant, V. Cherfaoui, and W. Yao, "Vehicle trajectory prediction based on motion model and maneuver recognition," in *2013 IEEE/RSJ International Conference on Intelligent Robots and Systems*, 2013, pp. 4363–4369.
- [44] M. Mizmizi, S. Mandelli, S. Saur, and L. Reggiani, "Robust and flexible tracking of vehicles exploiting soft map-matching and data fusion," in *2018 IEEE 88th Vehicular Technology Conference (VTC-Fall)*, 2018, pp. 1–5.
- [45] ITU-R, "Propagation by diffraction," International Telecommunication Union Radio Sector (ITU-R), Tech. Rep. P.526, 2019.
- [46] J. Goldhirsh and W. J. Vogel, "Handbook of propagation effects for vehicular and personal mobile satellite systems," *NASA Reference Publication*, vol. 1274, pp. 40–67, 1998.
- [47] M. Mizmizi, F. Linsalata, M. Brambilla, F. Morandi, K. Dong, M. Magarini, M. Nicoli, M. N. Khormuji, P. Wang, R. A. Pitaval, and U. Spagnolini, "Fastening the initial access in 5g nr sidelink for 6g v2x networks," *Vehicular Communications*, p. 100402, 2021. [Online]. Available: <https://www.sciencedirect.com/science/article/pii/S2214209621000711>
- [48] S. Lien, D. Deng, C. Lin, H. Tsai, T. Chen, C. Guo, and S. Cheng, "3gpp nr sidelink transmissions toward 5g v2x," *IEEE Access*, vol. 8, pp. 35 368–35 382, 2020.
- [49] M. T. Rahman, T. Karamat, S. Givigi, and A. Noureldin, "Improving multisensor positioning of land vehicles with integrated visual odometry for next-generation self-driving cars," *Journal of Advanced Transportation*, vol. 2018, 2018.
- [50] J. Ji, A. Khajepour, W. W. Melek, and Y. Huang, "Path planning and tracking for vehicle collision avoidance based on model predictive control with multiconstraints," *IEEE Transactions on Vehicular Technology*, vol. 66, no. 2, pp. 952–964, 2017.
- [51] M. Pfeiffer, G. Paolo, H. Sommer, J. Nieto, R. Siegwart, and C. Cadena, "A data-driven model for interaction-aware pedestrian motion prediction in object cluttered environments," in *2018 IEEE International Conference on Robotics and Automation (ICRA)*, 2018, pp. 5921–5928.
- [52] A. Jamakovic and S. Uhlig, "On the relationship between the algebraic connectivity and graph's robustness to node and link failures," in *2007 Next Generation Internet Networks*. IEEE, 2007, pp. 96–102.
- [53] R. E. Burkard and E. Cela, "Linear assignment problems and extensions," in *Handbook of combinatorial optimization*. Springer, 1999, pp. 75–149.
- [54] J. Wang, P. He, and W. Coo, "Study on the hungarian algorithm for the maximum likelihood data association problem," *Journal of Systems Engineering and Electronics*, vol. 18, no. 1, pp. 27–32, 2007.
- [55] S. Boyd, N. Parikh, E. Chu, B. Peleato, J. Eckstein *et al.*, "Distributed optimization and statistical learning via the alternating direction method of multipliers," *Foundations and Trends® in Machine Learning*, vol. 3, no. 1, pp. 1–122, 2011.
- [56] T. S. Rappaport, F. Gutierrez, E. Ben-Dor, J. N. Murdock, Y. Qiao, and J. I. Tamir, "Broadband millimeter-wave propagation measurements and models using adaptive-beam antennas for outdoor urban cellular communications," *IEEE Transactions on Antennas and Propagation*, vol. 61, no. 4, pp. 1850–1859, 2013.
- [57] M. R. Akdeniz, Y. Liu, M. K. Samimi, S. Sun, S. Rangan, T. S. Rappaport, and E. Erkip, "Millimeter wave channel modeling and cellular capacity evaluation," *IEEE Journal on Selected Areas in Communications*, vol. 32, no. 6, pp. 1164–1179, 2014.
- [58] 3GPP, "User equipment (ue) radio transmission and reception; part 2: Range 2 standalone," 3rd Generation Partnership Project (3GPP), Tech. Rep. TS 38.101, Oct. 2020.
- [59] ITU, "Effects of building materials and structures on radiowave propagation above about 100 mhz," International Telecommunication Union (ITU), Tech. Rep. ITU-R P.2040-1, May 2015.



Francesco Linsalata received B.Sc. and M.Sc. degrees cum laude in Telecommunication engineering from Politecnico di Milano, Milan, Italy, in 2017 and 2019, respectively. He is PhD student at the Dipartimento di Elettronica, Informazione e Bioingegneria, Politecnico di Milano. His main research interests focus on V2X communications and waveforms design for B5G wireless networks. He was the co-recipient of the best-paper award and recipient of the best student paper award at BalkanCom'19.



Silvia Mura received the M.Sc. degree in Telecommunication engineering from Politecnico di Milano, Milan, Italy, in 2020. She is a PhD student at the Dipartimento di Elettronica, Informazione e Bioingegneria, Politecnico di Milano. Her main research interests focus on signal processing in V2X communications.



Marouan Mizmizi is a post-doctoral research fellow at Dipartimento di Elettronica, Informazione e Bioingegneria, Politecnico di Milano, Italy, in the framework of Huawei-Polimi Joint Research Lab. He received the B.Sc. degree (2012), M.Sc. degree (2015) in Telecommunication Engineering and the Ph.D. (2019) in Information Technology from Politecnico di Milano. His research interests comprise advanced signal processing techniques for V2X communication systems, in particular for MIMO channel estimation in mmWave and sub-THz frequencies and Relay selection and scheduling in high mobility scenarios. He was the recipient of the Best Paper Award from the 29th International Conference on Advanced Information Systems Engineering, 2017.



Maurizio Magarini (M'04) received the M.Sc. and Ph.D. degrees in electronic engineering from the Politecnico di Milano, Milan, Italy, in 1994 and 1999, respectively. In 1994, he was granted the TELECOM Italia scholarship award for his M.Sc. Thesis. He worked as a Research Associate in the Dipartimento di Elettronica, Informazione e Bioingegneria at the Politecnico di Milano from 1999 to 2001. From 2001 to 2018, he was an Assistant Professor in Politecnico di Milano where, since June 2018, he has been an Associate Professor. From August 2008 to January 2009 he spent a sabbatical leave at Bell Labs, Alcatel-Lucent, Holmdel, NJ. His research interests are in the broad area of communication and information theory. Topics include synchronization, channel estimation, equalization and coding applied to wireless and optical communication systems. His most recent research activities have focused on molecular communications, massive MIMO, study of waveforms for 5G cellular systems, vehicular communications, wireless sensor networks for mission critical applications, and wireless networks using unmanned aerial vehicles and high-altitude platforms. He has authored and coauthored more than 120 journal and conference papers. He was the co-recipient of two best-paper awards. He is an Associate Editor of IEEE Access, IET Electronics Letters, and Nano Communication Networks (Elsevier). He has been involved in several European and National research projects.



Peng Wang received the Ph.D. degree in electronic engineering from the City University of Hong Kong, Hong Kong SAR, in 2010. He was a Research Fellow with the City University of Hong Kong from 2010 to 2012, and a Research Fellow with the University of Sydney, Australia, from 2012 to 2015. Since 2015, he has been with Huawei Technologies, Sweden, where he is currently a Senior Research Engineer. He has authored or co-authored over 60 peer-reviewed research papers in the leading international journals and conferences. His current research interests include 5G and beyond standardization, millimeter-wave communication, MIMO techniques, information theory and iterative multiuser detection. He received the Best Paper Award at the 2014 IEEE International Conference on Communications.



Majid Nasiri Khormuji received the Ph.D. degree in telecommunications from KTH—Royal Institute of Technology, Stockholm, Sweden in 2011. He held a visiting position at Stanford University, Stanford, CA in 2011. From 2011 to 2013, he was a Post-doctoral Research Fellow at the School of Electrical Engineering and the ACCESS Linnaeus Center at KTH. Since 2013, he is a Senior Researcher at Huawei Technologies Sweden AB in Stockholm, wherein he is conducting fundamental research for future wireless communication systems. Dr. Nasiri Khormuji has worked on problems in the area of network information theory, coding and transmission for wireless communications and statistical signal processing. He is the author of more than 50 journal and conference papers, some of which received best paper awards, and three chapters in books. He is also the inventor of numerous patent applications in a wide range of technologies spanning Multiple-Access, Modulation, Coding, MIMO, Massive MIMO and SWIPT. He has also served on the technical program committees for IEEE sponsored conferences including ICC, Globecom and WCNC.



Alberto Perotti is a Principal Research Engineer at Huawei Technologies, where he is involved in wireless networks' PHY layer research and standardization. He received his M.Sc. and Ph.D. degrees in telecommunications from Politecnico di Torino, Italy, in 1999 and 2003, respectively. Previously, he carried out research on mobile wireless and satellite communications at Politecnico di Torino. His interests cover coding and modulation, multiple access, and software-defined radios.



Umberto Spagnolini is Professor of Statistical Signal Processing, Director of Joint Lab Huawei-Politecnico di Milano and Huawei Industry Chair. His research in statistical signal processing covers remote sensing and communication systems with more than 300 papers on peer-reviewed journals/conferences and patents. He is author of the book *Statistical Signal Processing in Engineering* (J. Wiley, 2017). The specific areas of interest include mmW channel estimation and space-time processing for single/multi-user wireless communication systems, cooperative and distributed inference methods including V2X systems, mmWave communication systems, parameter estimation/tracking, focusing and wavefield interpolation for remote sensing (UWB radar and oil exploration). He was recipient/co-recipient of Best Paper Awards on geophysical signal processing methods (from EAGE), array processing (ICASSP 2006) and distributed synchronization for wireless sensor networks (SPAWC 2007, WRECOM 2007). He is technical experts of standard-essential patents and IP. He served as part of IEEE Editorial boards as well as member in technical program committees of several conferences for all the areas of interests.